Infrared Spectroscopy of Landau Levels of Graphene

Z. Jiang,[1,2,*] E. A. Henriksen,[1] L. C. Tung,[2] Y.-J. Wang,[2] M. E. Schwartz,[1] M. Y. Han,[3] P. Kim,[1] and H. L. Stormer[1,3,4]

[1]*Department of Physics, Columbia University, New York, New York 10027, USA*
[2]*National High Magnetic Field Laboratory, Tallahassee, Florida 32310, USA*
[3]*Department of Applied Physics and Applied Mathematics, Columbia University, New York, New York 10027, USA*
[4]*Bell Laboratories, Alcatel-Lucent, Murray Hill, New Jersey 07974, USA*

(Received 17 January 2007; published 11 May 2007)

We report infrared studies of the Landau level (LL) transitions in single layer graphene. Our specimens are density tunable and show *in situ* half-integer quantum Hall plateaus. Infrared transmission is measured in magnetic fields up to $B = 18$ T at selected LL fillings. Resonances between hole LLs and electron LLs, as well as resonances between hole and electron LLs, are resolved. Their transition energies are proportional to $\sqrt{B}$, and the deduced band velocity is $\tilde{c} \approx 1.1 \times 10^6$ m/s. The lack of precise scaling between different LL transitions indicates considerable contributions of many-particle effects to the infrared transition energies.

DOI: 10.1103/PhysRevLett.98.197403 PACS numbers: 78.66.Tr, 71.70.Di, 76.40.+b, 78.30.Na

Graphene is the newest member in the family of two-dimensional (2D) carrier systems, which have shown a spectrum of fascinating new physics over the past decades. Graphene, a single atomic sheet of graphite, represents the ultimate 2D material. Moreover, its electronic band structure differs radically from the parabolic bands common to all previous 2D systems. In graphene, the conduction and valence bands meet at two inequivalent, charge-neutral points in momentum space around which the dispersion is linear, leading to the so-called Dirac cones [1]. Much of the interest in graphene stems from an analogy of this dispersion relation to that of relativistic, massless fermions, leading to intriguing new phenomena. For instance, a very unusual half-integer quantum Hall effect (QHE) and a nonzero Berry's phase have been discovered in graphene [2–4], as well as an abnormally weak localization [5,6]. More recently, Raman spectroscopy [7–10] and angle resolved photoelectron spectroscopy [11] have been applied to graphene, yielding information on electron-phonon coupling and on the energy dispersion of the Dirac cones.

Infrared (IR) spectroscopy is a powerful tool for investigating the low-lying energy excitations of a material. When combined with a magnetic field B, it allows for the study of its Landau level (LL) spectrum. In traditional 2D materials with parabolic dispersions, this is tantamount to measuring the carrier effective mass m^*, since transitions between the equally spaced LLs at energy $E_n = (n + 1/2)\hbar eB/m^*$ reflect the same m^* as in classical cyclotron resonance at $\omega_c = eB/m^*$. Here e is the electron charge, $\hbar$ is Planck's constant, and the non-negative integer n is the LL index.

In a magnetic field, the linear dispersion relation of graphene leads to an unequally spaced LL spectrum [1,12,13]

$$E_n = \mathrm{sgn}(n)\sqrt{2e\hbar\tilde{c}^2B|n|} = \mathrm{sgn}(n)\sqrt{2|n|}\hbar\tilde{c}/l_0, \quad (1)$$

where $\tilde{c}$ is the band velocity, $l_0 = \sqrt{\hbar/eB}$ is the magnetic length, and $n > 0$ or $n < 0$ represents electrons or holes, respectively. Most unusually, for $n = 0$ there exists a LL at $E_0 = 0$ with a distinctive electron-hole degeneracy. This peculiar behavior of carriers in graphene is further enriched by spin splittings [4], possible lifting of the Dirac cone valley degeneracy, and general many-particle effects, and it provides a unique opportunity to probe these exceptional electronic properties of graphene via LL formation.

In this Letter, we report IR transmission results on single layer graphene. In fields up to $B = 18$ T, two identifiable resonances are clearly resolved, and their energy position scales as $\sqrt{B}$ with a slope corresponding to a $\tilde{c} \approx 1.1 \times 10^6$ m/s in Eq. (1). A deviation from an ideal ratio of $1:(\sqrt{2} + 1)$ between the two resonance energies, predicted by simple matrix elements [14], indicates a considerable many-particle contribution [15] to these LL transitions.

Sadowski *et al.* reported LL spectroscopy of ultrathin graphite layers created by thermal deposition on SiC [16]. Their data—at considerably lower magnetic field—also show $\sqrt{B}$ behavior, and they deduce a $\tilde{c}$ similar to ours. However, the nature of the thin graphite sheet remains unclear.

Our studies were performed on graphene, mechanically cleaved from bulk Kish graphite and deposited onto lightly doped Si/SiO_2 substrates [17], which are transparent to IR yet sufficiently conductive to serve as gates. The primary challenge of the experiment is the mismatch between the size of the IR focus in typical light-pipe systems (~1 mm) and the lateral dimension of typical mechanically extracted graphene samples (~10 μm). To overcome this limitation, we selected only large graphene specimens with areas as big as a few thousand μm^2 and employed a parabolic cone to focus the IR light to a few hundred μm spot. Standard e-beam lithography, metal evaporation, and lift-off techniques were used to define the Cr/Au (3/35 nm) contact wires, along with a ~100 μm diameter metal aperture around the specimen, which reduces stray IR light around the graphene sample; see the inset in Fig. 1. The graphene

device was mounted on the parabolic cone so the IR light passes through the Si substrate onto the graphene. The substrate was thinned and wedged to 4° to suppress Fabry-Perot interferences and could be aligned *in situ* with respect to the IR focus. A composite Si bolometer directly beneath the sample served as the IR detector. All electrical and IR experiments were performed at 4.2 K in magnetic fields up to $B = 18$ T using a conventional quasi-dc lock-in technique and a Bruker IFS 66v/S Fourier-transform infrared spectrometer.

The devices used in our work exhibit mobilities of $2–4 \times 10^3$ cm^2 V^{-1} s^{-1} measured at densities of $\sim 2 \times 10^{12}$ cm^{-2}. The gate voltage corresponding to charge neutrality V_{Dirac} is ~ 29 V due to a built-in potential from residual charges in the environment. Figure 1 shows a typical Hall resistance trace (R_{xy}) vs gate voltage for fixed $B = 18$ T taken *in situ*. The characteristic half-integer QHE with plateaus at $R_{xy} = h/\nu e^2$ for filling factors $\nu = \pm 2, \pm 6, \pm 10$ [2,3] is clearly observed, confirming the single layer nature of our graphene specimen.

We record IR transmission spectra at a fixed B field at two different carrier concentrations, corresponding to two different integer LL fillings. In this way, the experimental conditions are identical for all system components, such as bolometer sensitivity, silicon transparency, and B-induced shifts of the optical path. The only change is in the LL occupation of the graphene sample. Furthermore, since the LL spacing—and, hence, the IR resonance—is density (LL filling factor) dependent, the two spectra, although at an identical B field, show transmission minima at two different IR frequencies, and, thus, their ratio results in a maximum and a minimum placed on a background of 1. Figure 2 shows select transmission spectra of the sample shown in Fig. 1 at different magnetic fields following this normalization method, for two traces at filling factors $\nu = -2$ (numerator) and $\nu = -10$ (denominator). Given the fourfold LL degeneracy of graphene and the electron-hole symmetry of the $n = 0$ LL, filling factors $\nu = -2$ and $\nu = -10$ correspond to a Fermi level (E_F) position between the $n = -1$ and $n = 0$ LLs and the $n = -3$ and $n = -2$ LLs, respectively; see inset in Fig. 2. At $B = 18$ T, switching the gate voltages between these two positions tunes the hole density from 9.4×10^{11} to 4.7×10^{12} cm^{-2}.

Two transmission minima T_1 and T_2 are readily observable in the traces of Fig. 2. Their minima associate them with the $E_F(\nu = -2)$ position. Features from the $E_F(\nu = -10)$ position occur as maxima residing at lower energies and are visible only as shoulders in the 18 and 12.1 T traces. Therefore, in Fig. 2, the $E_F(\nu = -10)$ spectra simply serve as a normalization for the $E_F(\nu = -2)$ spectra.

Remaining artifacts in the data are largely due to 60 Hz harmonics (narrow spikes). In addition, a feature associ-

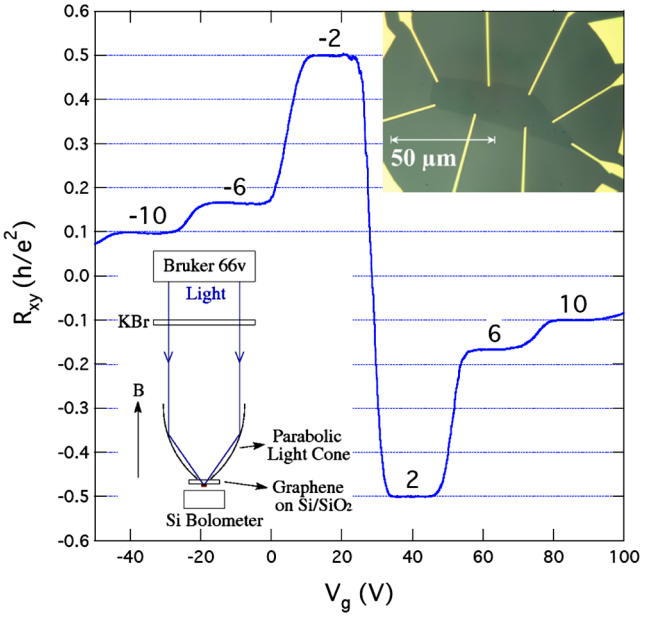

FIG. 1 (color online). Half-integer quantum Hall effect in graphene with plateaus at $R_{xy} = h/\nu e^2$ for filling factors $\nu = \pm 2, \pm 6, \pm 10$, at 4.2 K and 18 T. LL filling factors are indicated. Note that our devices are density tunable with $n_s/V_g = 7.2 \times 10^{10}$ cm^{-2} V^{-1}, where n_s is the charge carrier density in graphene. Upper inset: Optical image of an 1100 μm^2 graphene device. Lower inset: Schematic of the experimental setup.

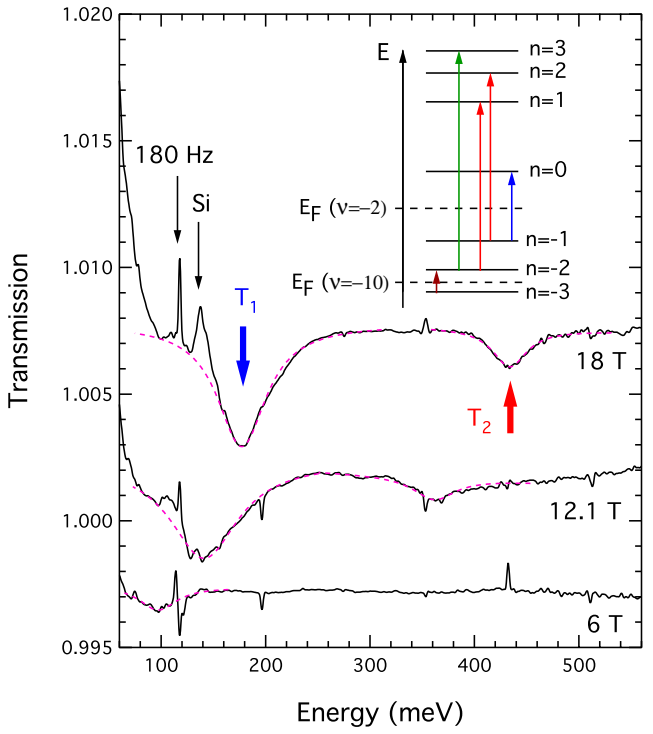

FIG. 2 (color online). Normalized IR absorption spectra of holes in graphene at three different magnetic fields, taken by dividing spectra taken at filling factors $\nu = -2$ and $\nu = -10$. Two LL resonances are denoted by T_1 and T_2. Residual spectral artifacts are associated with 60 Hz harmonics and with carriers in the Si substrate. Dashed purple lines are Lorentzian fits to the data. The inset shows a schematic LL ladder with allowed transitions indicated by arrows.

ated with the Si substrate emerges, since the introduction of carriers in graphene leads to the same density but opposite sign of carriers at the Si-SiO_2 interface [18]. The transmission of this carrier system is density dependent and therefore does not completely average out in spectral division. However, these artifacts in Fig. 2 can be circumvented, and we find that the minima can be fit well by a Lorentzian, shown by the dashed lines. From these fits, we determine the resonance position and the half-width of each resonance.

The transmission minima in Fig. 2 are well developed, and their resonance energies clearly decrease with decreasing magnetic field. Evidently, T_2 is considerably weaker than T_1, and the ratio of their intensities seems to be roughly constant. The widths of the resonances δE are similar for T_1 and T_2 and correspond to a scattering time $\tau \cong \hbar/\delta E \cong 20$ fs in reasonable agreement with $\tau \cong 40$ fs, derived from the mobility.

Figure 3(a) summarizes the energies of the T_1 and T_2 transitions determined from Lorentzian fits to spectra from holes (Fig. 2) and electrons (not shown), plotted as a function of $\sqrt{B}$. A clear $\sqrt{B}$ relationship emerges. This dependence is very reliable for the T_1 transition with a large

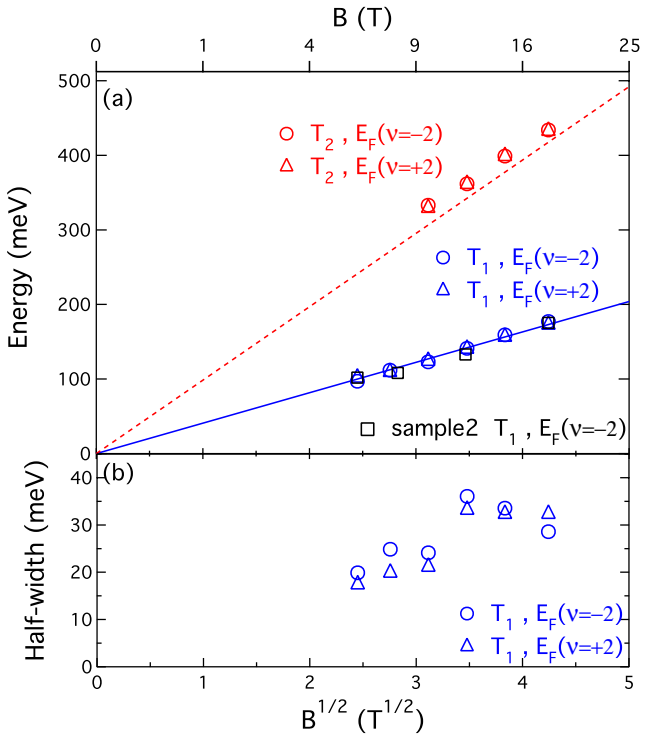

FIG. 3 (color online). (a) Resonance energies vs $\sqrt{B}$, from holes (ratio of $\nu = -2$ and $\nu = -10$ data, Fig. 2) and electrons (ratio of $\nu = +2$ and $\nu = +10$, spectra not shown). Similar behavior has been observed in a second sample (squares). The solid line is a best $\sqrt{B}$ fit to the T_1 transition, yielding $\tilde{c} = (1.12 \pm 0.02) \times 10^6$ m/s. The dashed line represents a scaling of the solid line by a factor of $(\sqrt{2} + 1)$. (b) Half width at half maximum from Lorentzian fits of the T_1 transitions, as a function of $\sqrt{B}$.

number of data points to a low B field. According to Eq. (1), a $\sqrt{B}$ dependence is expected for any transition between LLs in graphene, and our data confirm this. Inspecting the slope and comparing it with Eq. (1), assuming $\tilde{c} \approx 1 \times 10^6$ m/s [2,3,19,20], identifies the transition as the $n = -1 \rightarrow n = 0$ (holes) and $n = 0 \rightarrow n = 1$ (electrons) intraband LL transitions. Quantitatively, this assignment leads to a refined value of $\tilde{c} = (1.12 \pm 0.02) \times 10^6$ m/s, indicated as a line through the data in Fig. 3(a). Given the Fermi level position $E_F(\nu = -2)$ shown in the inset in Fig. 2, these are the lowest LL transitions possible in graphene. Figure 3(b) shows the B dependence of the half width at half maximum of transition T_1. It seems to be increasing, but its B dependence cannot be further assessed at this stage.

Had this been a traditional 2D electron or hole system, we would have observed only one resonance line, the cyclotron resonance at $\hbar\omega_c = \hbar eB/m^*$, from which arises a unique mass m^*. In contrast, we observe a second, higher energy transition T_2. To identify the LLs involved requires a recapitulation of the relevant dipole transition selection rules. In a traditional 2D system with energy spectrum $E_n = (n + 1/2)\hbar\omega_c$, they dictate $\Delta n = n_2 - n_1 = \pm 1$ for either electron or hole Landau ladders. When expanded to semiconductors in which interband transitions from a hole LL n_h to an electron LL n_e are also feasible, the selection rule changes to $\Delta n = n_e - n_h = 0$ due to the separate p and s character of the valence and conduction band. In graphene, in which the ''valence'' and ''conduction band'' have the same symmetry, a single selection rule $\Delta n = |n_2| - |n_1| = \pm 1$ is obtained [14] for intra- as well as for interband transitions. Therefore, the next allowed LL transitions for $E_F(\nu = -2)$ with energy above the $n = -1 \rightarrow n = 0$ transition are interband transitions $n = -2 \rightarrow n = 1$ and $n = -1 \rightarrow n = 2$; see the inset in Fig. 2. While preserving the general $\sqrt{B}$ dependence, their energy scales as $1{:}(\sqrt{2} + 1)$ compared to the $n = -1 \rightarrow n = 0$ intraband transition, following Eq. (1). The dashed line in Fig. 3(a) represents a scaling of the T_1 transition by a factor of $\sqrt{2} + 1$ and falls quite close to the T_2 data. This provides very good evidence that T_2 represents the lowest interband transition expected from the inset in Fig. 2 and its electron-hole symmetric equivalent.

The observed small deviation of the $1{:}(\sqrt{2} + 1)$ ratio of the T_1 and T_2 energies, however, lies well outside of the experimental errors ($\leq$symbol size). A $\sqrt{B}$ fit to T_2 with a zero energy intercept results in $\tilde{c} = (1.18 \pm 0.02) \times 10^6$ m/s, according to Eq. (1). This value differs appreciably from the value $\tilde{c} = (1.12 \pm 0.02) \times 10^6$ m/s deduced from T_1, as well as from the value of $\tilde{c} = (1.03 \pm 0.01) \times 10^6$ m/s found by Sadowski *et al.* [16], who derive the same band velocity $\tilde{c}$ for both transitions.

The discrepancy between the band velocities deduced from different LL transitions sheds doubt on the applicability of a simple LL energy subtraction scheme based on Eq. (1) for the interpretation of IR data in graphene. In 2D

systems with parabolic dispersions, Kohn's theorem [21] explains that *e-e* interactions have no impact on the LL transition energies observed in IR experiments (cyclotron resonance). Instead, the resonance energy coincides with the noninteracting value, provided that the system is translationally invariant, which, in spite of residual disorder, can largely be assumed to hold. Yet, Kohn's theorem fails in the case of graphene, whose linear dispersion may be viewed as a case of extreme nonparabolicity, and thus many-particle effects may be expected to contribute to the LL transition energies.

Indeed, the first calculations of many-particle corrections to the bare LL transitions are appearing in the literature. A recent paper by Iyengar *et al.* [15] arrives at quite large many-particle contributions, on the order of a few $e^2/\epsilon l_0 = 56\ \mathrm{meV}\sqrt{B(T)}/\epsilon$, which amounts to an energy of $\sim$60 meV at $B = 18$ T with an assumed dielectric constant of $\epsilon = 4$. Importantly, the total transition energy between LLs with indices n and m scales as $\Delta E_{n,m} l_0 = \sqrt{2}\hbar\tilde{c}(\sqrt{|m|} \pm \sqrt{|n|}) + C_{n,m} e^2/\epsilon$, so that contributions from $\tilde{c}$ and $C_{n,m}/\epsilon$ cannot be distinguished by their B dependence.

On the other hand, the magnitude of the many-particle effects $C_{n,m}$ depends on the specific n, m LL pair, a fact that can be employed to distinguish them from the band velocity contribution $\tilde{c}$. Iyengar *et al.* [15,22] calculated the prefactors $C_{-1,0} = 1.18$ and $C_{-2,1} = C_{-1,2} = 3.17$ for the transitions T_1 and T_2 of Fig. 3(a), respectively. Since $C_{-2,1}/C_{-1,0} > (\sqrt{2} + 1)$, any *e-e* contribution to the LL transition will increase the ratio of transition energies beyond its noninteracting value of $\sqrt{2} + 1$, as is observed in our data. In fact, a band velocity $\tilde{c} \approx 8 \times 10^5$ m/s and $\epsilon \approx 5$ can fit simultaneously the T_1 and T_2 data of Fig. 3(a). However, at this stage a wide range of $\tilde{c}$ and ϵ produce similar good fits within the error bars of the experiment, making it premature to assign any particular values. More precise IR measurements between several other, higher LLs are required to assess quantitatively the impact of many-particle physics on these transitions. At this stage, it appears likely that a determination of the band velocity from a single particle LL picture leads to a considerable overestimation of its value. A quantitative comparison of our data with many-body calculations [15,22] may be premature, since theory does not take into account disorders [23,24] nor any mesoscopic corrugations of the graphene sheet [5].

Finally, apart from many-particle effects, one may wonder as to the impact of a possible gap opening around the Dirac point due to interaction effects, a scenario that has been addressed by Gusynin *et al.* [14]. In this model, any positive value for the gap energy reduces the ratio of T_2 to T_1 below $\sqrt{2} + 1$, in contrast to our data.

In summary, we have observed intra- and inter-LL transitions in IR spectroscopy on graphene. The transition energies scale as $\sqrt{B}$ and a simple, noninteracting LL transition interpretation yields a band velocity of $\tilde{c} \approx 1.1 \times 10^6$ m/s. The observed deviation from a precise $1{:}(\sqrt{2} + 1)$ scaling between the transition energies indicates a contribution from many-particle interactions to the transitions. Theory predicts rather strong ($\sim$30%) such corrections [15,22]. Qualitatively, the observed deviations show the correct sign, but the magnitude of the corrections cannot yet be deduced reliably from experiment.

We thank Kun Yang, H. A. Fertig, L. Brey, Jianhui Wang, and D. N. Basov for discussions and B. Oezyilmaz for assistance in fabrication. This work is supported by the DOE (No. DE-AIO2-04ER46133 and No. DE-FG02-05ER46215), NSF (No. DMR-03-52738 and No. CHE-0117752), NYSTAR, and the Keck Foundation. IR measurement of this work was performed at the National High Magnetic Field Laboratory, which is supported by NSF Cooperative Agreement No. DMR-0084173, by the State of Florida, and by the DOE. We thank J. Jaroszynski, E. C. Palm, T. P. Murphy, S. W. Tozer, and B. L. Brandt for experimental assistance. Z. J. and E. A. H. contributed equally to this work.

*Electronic address: jiang@magnet.fsu.edu

[1] J. W. McClure, Phys. Rev. **104**, 666 (1956).
[2] K. S. Novoselov *et al.*, Nature (London) **438**, 197 (2005).
[3] Y. Zhang *et al.*, Nature (London) **438**, 201 (2005).
[4] Y. Zhang *et al.*, Phys. Rev. Lett. **96**, 136806 (2006).
[5] S. V. Morozov *et al.*, Phys. Rev. Lett. **97**, 016801 (2006).
[6] Xiaosong Wu *et al.*, Phys. Rev. Lett. **98**, 136801 (2007).
[7] A. C. Ferrari *et al.*, Phys. Rev. Lett. **97**, 187401 (2006).
[8] D. Graf *et al.*, Nano Lett. **7**, 238 (2007).
[9] J. Yan *et al.*, Phys. Rev. Lett. **98**, 166802 (2007).
[10] Simone Pisana *et al.*, arXiv:cond-mat/0611714.
[11] Aaron Bostwick *et al.*, arXiv:cond-mat/0609660.
[12] F. D. M. Haldane, Phys. Rev. Lett. **61**, 2015 (1988).
[13] G. W. Semenoff, Phys. Rev. Lett. **53**, 2449 (1984).
[14] V. P. Gusynin, S. G. Sharapov, and J. P. Carbotte, Phys. Rev. Lett. **98**, 157402 (2007).
[15] A. Iyengar *et al.*, Phys. Rev. B **75**, 125430 (2007).
[16] M. L. Sadowski *et al.*, Phys. Rev. Lett. **97**, 266405 (2006).
[17] K. S. Novoselov *et al.*, Proc. Natl. Acad. Sci. U.S.A. **102**, 10 451 (2005).
[18] N. Sai *et al.*, Phys. Rev. B **75**, 045307 (2007).
[19] M. S. Dresselhaus and G. Dresselhaus, Adv. Phys. **51**, 1 (2002).
[20] N. B. Brandt, S. M. Chudinov, and Y. G. Ponomarev, *Semimetals 1: Graphite and Its Compounds* (North-Holland, Amsterdam, 1988).
[21] W. Kohn, Phys. Rev. **123**, 1242 (1961).
[22] Jianhui Wang and H. A. Fertig (private communication).
[23] N. M. R. Peres, F. Guinea, and A. H. C. Neto, Phys. Rev. B **73**, 125411 (2006).
[24] Balázs Dóra and Peter Thalmeier, arXiv:cond-mat/0701714.